Multinuclear Solid-State High-Resolution and^{13}C -{^{27}Al} Double-Resonance Magic-Angle Spinning NMR Studies on Aluminum Alkoxides

Anuji Abraham, Roel Prins, and Jeroen A. van Bokhoven*

Institute for Chemical and Bioengineering, Swiss Federal Institute of Technology (ETH), Zurich 8093, Switzerland

Ernst R. H. van Eck* and Arno P. M. Kentgens

Department of Physical Chemistry - Solid-State NMR, Institute for Molecules and Materials, Radboud University of Nijmegen, Toernooiveld 1, 6525 ED Nijmegen, Netherlands

Received: September 7, 2005; In Final Form: January 20, 2006

A combination of ^{27}Al magic-angle spinning (MAS)/multiple quantum (MQ)-MAS, ^{13}C−^{1}H CPMAS, and ^{13}C−{^{27}Al} transfer of population in double-resonance (TRAPDOR) nuclear magnetic resonance (NMR) were used for the structural elucidation of the aluminum alkoxides aluminum ethoxide, aluminum isopropoxide, and aluminum tertiarybutoxide. Aluminum alkoxides exist as oligomers with aluminum in different coordinations. High-resolution ^{27}Al MAS NMR experiments with high-spinning speed distinguished the aluminum atoms in different environments. The ^{27}Al MAS NMR spectrum gave well-resolved powder patterns with different coordinations. *Z-filter* MQ-MAS was performed to obtain the number and types of aluminum environments in the oligomeric structure. ^{13}C−^{1}H CPMAS chemical shifts resolved the different carbon species (−CH_3, =CH_2, =CH−, and =C=) in the structures. ^{13}C−{^{27}Al} TRAPDOR experiments were employed to obtain relative Al−C dipolar interactions and to distinguish between terminal and bridging alkoxides in the crystallographic structures. The complete characterization of selected aluminum alkoxides using advanced NMR methods has evidenced the tetrameric structure for aluminum isopropoxide and the dimeric structure for aluminum tertiary-butoxide, as reported in the literature, and proposed a polymeric structure for aluminum ethoxide.

Introduction

Alkoxides are compounds containing acceptor and adjacent donor centers in the same molecule and are capable of forming adducts between molecules to give oligomers such as dimers, trimers, or tetramers.[1−4] The aluminum ion (Al^{3+}) is chemically flexible enough to form four-, five-, and six-coordinated complexes. Therefore, alkoxides form adducts with aluminum atoms, which can be in four, five, or six coordination or mixed coordinations, to form aluminum alkoxide oligomers. Double alkoxides, such as aluminum siloxides with Al−O−Si linkages, are used as precursors for the synthesis of aluminosilicate ceramics.[5] Thus, a structural characterization of these compounds is important due to its close relationship with chemical reactivity.

Aluminum alkoxide compounds are sensitive to air and moisture. As a result, there are some studies[3,6−12] on the structure of these compounds but very few studies[1,10,13−17] on the structural elucidation of these materials by nuclear magnetic resonance (NMR) methods. These systems have certainly not been studied by means of solid-state NMR techniques. ^{13}C and ^{1}H liquid-state NMR studies provide valuable structural information,[10,14] but ^{27}Al liquid-state NMR studies[1,15] have not been equally successful due to the broad lines in the spectrum, giving difficulties in assigning the isotropic chemical shifts. Another reason for the lack of meaningful solid-state NMR information for these materials is the unavailability of high-field magnets and high-spinning speeds in the past. Now, high-field magnets and high-spinning speeds have made NMR the *state-of-the-art* technique for studying quadrupolar nuclei with very large quadrupolar broadening. Aluminum is a quadrupolar nucleus with a spin of 5/2. The ^{27}Al magic-angle spinning (MAS) spectrum of a perfectly crystalline material gives powder patterns with very large second-order quadrupolar broadenings. It is very important to have high fields and high-spinning speeds to obtain a powder pattern in which the centerband does not overlap with the spinning sidebands. Furthermore, the development of solid-state NMR for measuring heteronuclear dipolar interactions has had a large impact on the study of solids as in the current work.

The crystal structures of two of the compounds under study are known from X-ray diffraction studies. Advantages of NMR over X-ray diffraction occur in cases where only amorphous and/or mixed-phase (amorphous and crystalline) materials can be studied. In the case of crystalline compounds, NMR can still provide supporting information for the structural elucidation, especially when only powder diffraction is feasible if crystals of sufficient size are lacking.

Here, we present a combination of ^{27}Al MAS, ^{27}Al *z-filter*[18] multiple quantum (MQ)-MAS,[19,20] ^{13}C−^{1}H CPMAS, and ^{13}C−{^{27}Al} transfer of population in double-resonance (TRAPDOR)[21−24] (Figure 1) NMR techniques for the characterization of a number of aluminum alkoxides: aluminum ethoxide, aluminum isopropoxide, and aluminum *tert*-butoxide. The MQ-MAS is instrumental in obtaining high-resolution NMR spectra of half-integer quadrupolar spins. This two-dimensional experiment correlates the central $<1/2|-1/2>$ transition with

* To whom correspondence should be addressed. E-mail: j.a.vanbokhoven@chem.ethz.ch; E.vanEck@nmr.ru.nl.

10.1021/jp055058k CCC: $33.50
Published on Web 03/15/2006

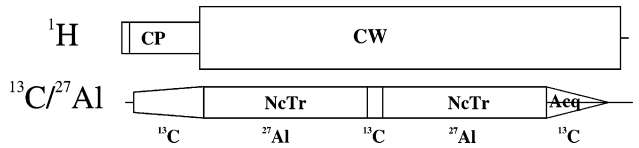

Figure 1. TRAPDOR pulse sequence, including cross polarization and decoupling. Spectrometer was operated as a 3-channel machine, however the C and Al channels were combined using a combiner/splitter before being fed into the high-power amplifier. CP: cross-polarization time; Nc: number of rotor periods; Tr: pulse length; Acq: acquisition time.

the symmetric $<n/2|-n/2>$ multiple-quantum transition ($n = 3$, 5, 7, or 9). The second-order quadrupolar interaction affects both transitions with the same angular dependencies except for a scaling factor. The result is a two-dimensional spectrum where the peaks appear as ridges that, after a shearing transformation, will give isotropic spectra along the F1 dimension and spectra displaying the normal second-order quadrupolar line shapes along F2.

With the TRAPDOR experiment, one can assess the strength of the dipolar interaction between different nuclei. The dipolar interaction gives information about the internuclear distance and is proportional to $1/r^3$. In this experiment, a rotor-synchronized echo is observed on spin *I*, and its intensity is compared with an experiment in which the other nucleus, spin *S*, is irradiated during the echo period. The *S* spin should be a quadrupolar nucleus so that the RF irradiation in combination with the spinning will induce rotor-synchronous level crossings on the *S* spins. This will result in a similar effect on spin *I*, as in a REDOR experiment; namely, the *IS* dipolar couplings are periodically altered and will diminish the echo intensity. Those *I* spins in contact with *S* spins will dephase, even more so for longer times and/or stronger couplings. This experimentally obtained dipolar moment can be used to obtain internuclear distances, or in more complex situations with multiple spins present, this can be compared with theoretically calculated second moments on the basis of a structural model.[25] The $^{13}C-\{^{27}Al\}$ TRAPDOR NMR technique has been applied to other systems, such as aluminum lactate, aluminum acetylacetonate, and hydroxyl aluminum diacetate, to determine the aluminum−carbon (Al−C) distances.[23] Other systems in which Al−C bonds are relevant are zeolites, which are used as catalysts and catalyst supports. The preparation of zeolites and related structures is based on organic template molecules, and in catalysis, organic reactants containing carbon atoms are adsorbed on the active sites of aluminum-containing zeolites.[21,22] Their structural characterization gives information about the structure−performance relationship of these systems. In this respect, this work functions as a feasibility study for addressing such structural investigations.

Experimental Section

The aluminum alkoxides, aluminum ethoxide, aluminum isopropoxide, and aluminum tertiary-butoxide were obtained from Aldrich with 98% purity without any isotope enrichment. These alkoxides are very sensitive to moisture in the air and will rapidly hydrolyze if exposed. Therefore, the samples were packed in 2.5-mm PENCIL rotors in a glovebox in a dry nitrogen atmosphere, and sample spinning was also done using dry nitrogen gas.

All of the NMR experiments were carried out on a Chemagnetics CMX-Infinity 600 Solid-State NMR spectrometer, operating at a magnetic field strength of 14.1 T. A Chemagnetics 2.5 mm H−X double-resonance APEX probe was used. Modification of the same probe allowed its use for $^{13}C-^{27}Al-^{1}H$ triple resonance (vide infra). The resonance frequencies were 150.87 MHz for ^{13}C, 156.34 MHz for ^{27}Al, and 599.99 MHz for ^{1}H. The magnet was shimmed on adamantane to a line-width of less than 6 Hz. Adamantane was also used as an external reference for ^{13}C by setting the CH_2 resonance to 38.7 ppm.

For the CPMAS experiment, the magnetization was transferred from protons to carbons using variable amplitude cross polarization (VACP). RF field strengths of 51 kHz were applied on ^{13}C and on ^{1}H, and a linear ramp of 2 kHz centered around 61 kHz was used. CP was at the −1 Hartman−Hahn sideband condition at an MAS frequency of 10 kHz. The contact time for cross polarization was set to 0.25 ms for aluminum ethoxide and aluminum isopropoxide and 4 ms for the aluminum *tert*-butoxide sample. A recycle delay of 5 s was sufficient to restore the proton magnetization to equilibrium. During acquisition, the protons were decoupled using the XiX decoupling scheme[26] with 285-μs pulse lengths.

For the ^{27}Al single-pulse MAS and ^{27}Al 3Q-MAS NMR experiments, a 1 M aqueous solution of aluminum nitrate was used to determine the RF field strengths and to serve as an external reference at 0 ppm. Single-pulse spectra were obtained at spinning speeds of 22.5 kHz and recycle delays of 0.4 s (at least $3T_1$). Typically, 1024 FIDs were accumulated using a spectral width of 250 kHz and a dead time delay of 8 μs. The 1.0-μs excitation pulse employed an RF power of 40 kHz, well within the weak RF regime ($\nu_{RF} \ll \nu_Q$) for all the resonances, thus ensuring that the relative peak intensities were quantitative.[27]

The ^{27}Al 3Q-MAS[19,20] experiments were performed using the three-pulse *z-filter*[18] sequence. Signal acquisition was done using the hyper-complex States procedure.[28] Pulses of 1.3- and 0.45-μs duration, at an RF field strength of 310 kHz, were used for the creation of triple quantum coherence and the conversion ($\pm 3Q \rightarrow 0Q$) pulses, respectively. Typically, the indirect dimension was sampled with 128-μs increments, resulting in a 125 kHz spectral width in F1. The *z-filter* ($0Q \rightarrow -1Q$) is a central transition selective soft 90° pulse, which lasted for 4 μs with 21 kHz of RF power. A two-dimensional (2D) Fourier transformation followed by a shearing transformation[20,29] gave a pure absorption mode 2D contour plot where the one-dimensional (1D) projection of the 2D contour plot onto the F1 axis gives the isotropic spectra.

To perform the $^{13}C-\{^{27}Al\}$ TRAPDOR (Figure 1) experiments, the quality factor (Q) of the X channel of the double-resonance probe was reduced to about 23 by putting a 3 kΩ resistance in parallel with the tuning insert capacitor. The X channel of the probe was tuned to −8.2 dB at 152.9 MHz, resulting in a reflected power of −5.0 and −3.8 dB at 150.8 and 156.3 MHz, respectively. As a comparison, the unmodified probe has a Q of about 100 and a reflected power of better than −30 dB. The tuning of the proton channel was not affected by these modifications. The spectrometer itself was set up as a standard three-channel machine; however, the carbon and aluminum channels were both fed into the same amplifier using a splitter-combiner and then connected to the X channel. In this way, RF field strengths of 59 kHz were attained for ^{13}C at 175 W RF power, 40 kHz for ^{27}Al at 83 W RF power, and 64 kHz for ^{1}H at 16 W RF power. TRAPDOR experiments on aluminum *tert*-butoxide were performed with these power levels at 5 kHz MAS and with CW proton decoupling. VACP was used with a 2 kHz linear ramp on protons to transfer the magnetization from protons to carbon in 2-ms contact time. For the aluminum ethoxide and aluminum isopropoxide samples, TRAPDOR

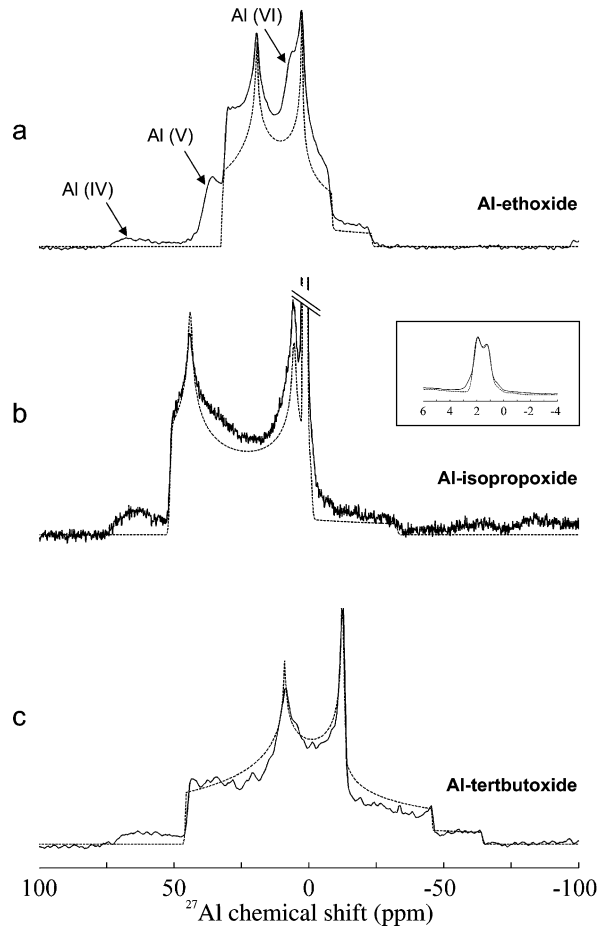

Figure 2. ^{27}Al MAS NMR spectra of the aluminum alkoxides (a) aluminum ethoxide, (b) aluminum isopropoxide, and (c) aluminum *tert*-butoxide at MAS speeds of 22 kHz. Dashed lines are simulations using the parameters from Table 1. Alumina resonances are present in all samples and are indicated in the aluminum ethoxide spectrum.

experiments were performed at 10 kHz MAS using VACP of 61 kHz on ^{1}H and 51 kHz on ^{13}C in 0.25-ms duration contact time. Proton CW decoupling of 124 kHz was used during the echo and acquisition. The aluminum was irradiated with a 93 kHz strong RF field. The intensity of the rotor-synchronized ^{13}C echo was monitored as a function of the number of rotor periods (up to 192). The effect of the aluminum irradiation on the echo intensity was normalized by acquiring a full echo without aluminum irradiation for each echo time. The spinning speed was stable within 1 Hz; hence, rotor-synchronization could easily be accomplished by setting the timings to their appropriate values.

All data were processed using the matNMR processing software.[30] On basis of the position of the lines along the triple quantum dimension 2D 3QMAS spectra and the center of gravity of the lines as determined from the 1D spectra, the quadrupolar product $P_Q = C_Q(1+\eta^2/3)$ and the isotropic chemical shift of all the resonances were determined. From the 1D spectra, the quadrupole coupling C_Q constant, the asymmetry parameter (η), as well as the isotropic chemical shift were determined by simulating the quadrupolar line shapes using the parameters obtained from the MQ spectra as starting values.

Results

Figure 2 shows the ^{27}Al MAS spectra of all samples including the simulations. All the spectra exhibit distinctive second-order quadrupolar powder patterns as well as some low-intensity peaks representing hydrolyzed alkoxide. The spectra of both the aluminum ethoxide (Figure 2a) and the aluminum *tert*-butoxide (Figure 2c) display a single quadrupolar line shape (in addition to the aforementioned featureless resonances of the hydrolyzed product). The ^{27}Al MAS spectrum of aluminum isopropoxide (Figure 2b) shows two quadrupolar line shapes, a broad and a relatively narrow one (inset), with an intensity ratio of 3:1. Triple quantum 2D MAS spectra resolved the overlapping peaks. Figure 3 shows the ^{27}Al 3QMAS NMR spectra of all the samples. Cross sections along F2 are taken for all resonances, including the ± 1 spinning sidebands in F1. The quadrupole parameters and isotropic shifts extracted from the 1D and 2D data are listed in Table 1. The isotropic chemical shift of 35.5 ppm for aluminum ethoxide is in the pentacoordinated region. The ^{27}Al isotropic chemical shifts of 61.5 and 2.5 ppm for aluminum isopropoxide are in the tetrahedral and octahedral regions, respectively. The isotropic chemical shift of 48.5 ppm for aluminum *tert*-butoxide is in the tetrahedral region. The signal from the hydrolyzed product is present in the MQ-MAS spectra, but because of a distribution in quadrupole parameters, their intensity is distributed over a large area so that they do not show up in the contour plots.

Figure 4 shows the ^{13}C CPMAS spectra of the samples, and Table 2 lists the isotropic chemical shifts. The carbon spectrum of aluminum ethoxide (Figure 4a) exhibits 3 resonances in the methyl ($-CH_3$) region between 15 and 22 ppm and a resonance at 59.6 ppm, attributed to the methylene carbon attached to the oxygen atom ($-OCH_2-$). Figure 4a (inset) indicates that this line actually consists of 2 overlapping resonances, which are not from the experimental shortcomings such as poor shimming. The ^{13}C CPMAS spectrum of the aluminum isopropoxide (Figure 4b) shows 2 resonances of equal integrated intensity in the alkoxy-carbon region, and the inset shows 11 resonances in the methyl-carbon region. Of the methyl resonances, the most shielded peak at 25.5 ppm has twice the intensity of the other methyl resonances. The remaining 10 methyl resonances are distributed between 25.8 and 29.9 ppm and have roughly equal intensity. Therefore, a total of 12 methyl groups can be discerned. The ^{13}C CPMAS spectrum of aluminum *tert*-butoxide shows extremely narrow lines (Figure 4c). There are 3 resonances of equal intensity both for the alkoxy carbons and for the methyl carbons. The alkoxy carbons give a closely spaced doublet, whereas one of the peaks is shifted to a higher frequency (76.7 ppm). For the methyl carbons, we also observe a doublet, whereas the third line is shifted to a lower frequency (32.5 ppm). The intensities for the alkoxy carbons are significantly lower than those of the methyl carbons. This is due to the reduced efficiency of the cross polarization because no protons are attached directly to these alkoxy carbons.

^{13}C$-\{^{27}$Al$\}$ TRAPDOR curves were obtained for the samples aluminum ethoxide and aluminum *tert*-butoxide (Figure 5). For aluminum ethoxide, the TRAPDOR fraction, which is the loss in signal intensity relative to the full echo intensity, is displayed in Figure 5a for each of the four ^{13}C resonances. A stronger TRAPDOR effect was observed for the $-OCH_2-$ carbon peak at 59.6 ppm than for the three methyl-carbon peaks, all of which showed similar dipolar dephasing. As a comparison, the solid curves are theoretical REAPDOR dephasing curves calculated using:

$$S^{\mathrm{REAP}}_{1/2,5/2}(nTrD) = 0.63(1 - \exp(-(3.0nTrD)^2) + 0.2(1 - \exp(-(0.7nTrD)^2)$$

which was introduced by Goldbourt et al.[31] Here, $S^{\mathrm{REAP}}_{1/2,5/2}(nTrD)$

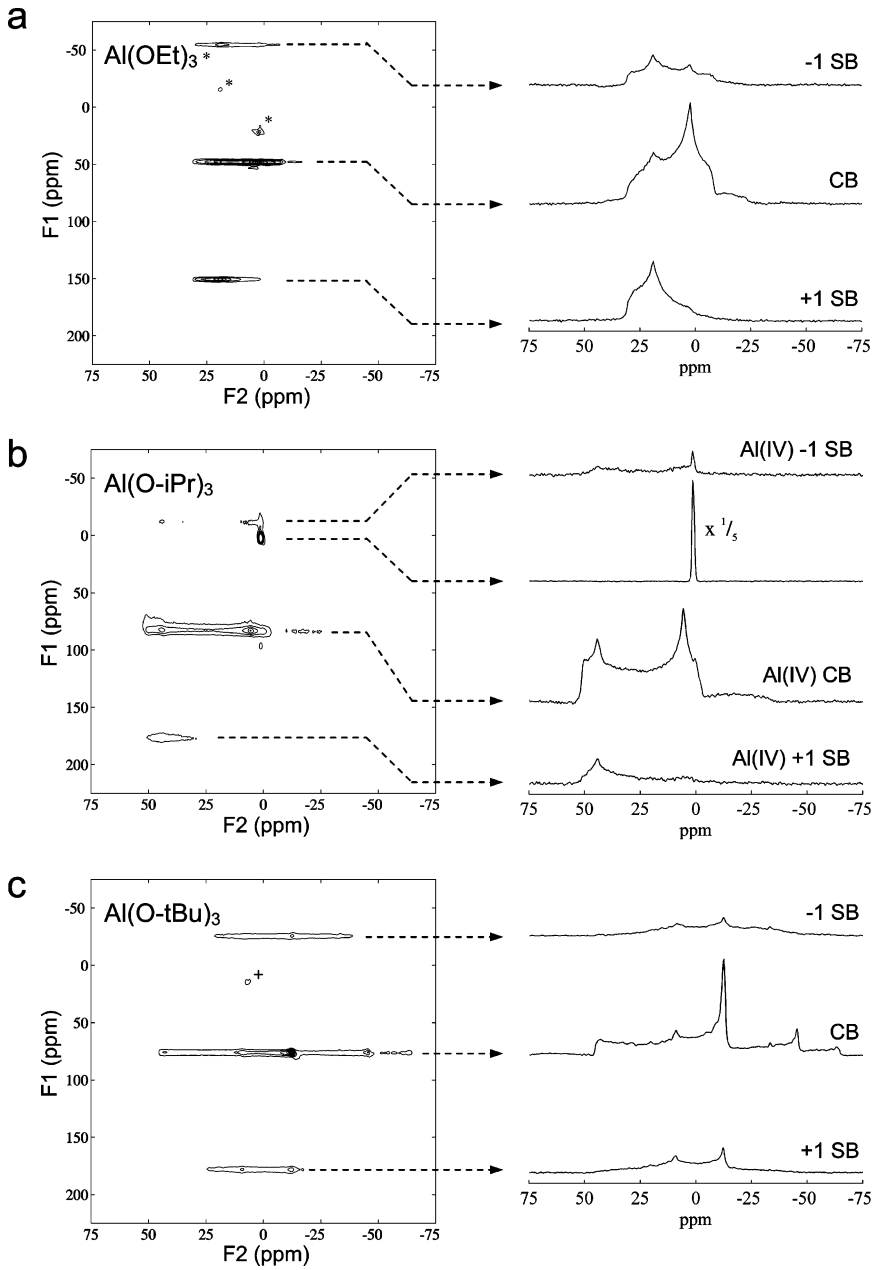

Figure 3. ^{27}Al 3QMAS NMR sheared spectra of (a) aluminum ethoxide, (b) aluminum isopropoxide, and (c) aluminum *tert*-butoxide. On the right of each 2D spectrum are slices through the main peaks as well as through the ±1 spinning sidebands. Height of the slice through the octahedral aluminum in the aluminum ethoxide (b) was reduced by a factor 5. A "+" indicates hydrolyzed material, and "*" indicates an artifact.

TABLE 1: ^{27}Al Isotropic Chemical Shifts and Quadrupole Parameters, Determined from Simulation of 1D Data (Normal) and Peak Positions in 3QMAS Spectra (Italic)

	δ_{iso} (ppm)		C_Q (MHz)	η	P_Q (MHz)	δ_{iso} (ppm)
Al−ethoxide	35.5	(35.9)[a]	9.65	0.39	*9.7*	*34*
Al−isopropoxide (IV)	61.5	(64.3)[a]	12.37	0.14	*13.1*	*58*
(VI)	2.5	(3.2)[a]	1.9	0	*1.4*	*2*
Al−*tert*-butoxide	48.5	(48.5)[a]	13.14	0.61	*13.8*	*49*
Al_2O_3 (IV)					*6.0*	*73*
(V)					*5.6*	*42*
(VI)					*5.2*	*11*

[a] Solution NMR data from ref 1.

would be the TRAPDOR fraction where *nTr* is the total echo time and *D* is the IS dipolar coupling, given by $D = (\mu_0/4\pi)\hbar\gamma_I\gamma_S/2\pi r^3$ (Hz). Although the curves were calculated for the REAPDOR experiment, they can still be used to qualitatively describe the TRAPDOR experiment because both experiments rely on the changes in the spin state of the quadrupole nucleus induced by the combination of MAS the application of an RF field. ^{13}C−{^{27}Al} TRAPDOR curves for aluminum *tert*-butoxide are shown in Figure 5b; the intensities for the paired peaks at 34.8 and 34.5 ppm and at 69.2 and 69.3 ppm were taken together (similar behavior as well as overlap). For each type of carbon, two distinct TRAPDOR behaviors can be seen: a strongly coupled carbon resonance and more weakly coupled carbon resonances. The strongly coupled peaks are the isolated peaks at 32.5 ppm for the methyl carbons and at 76.7 ppm for the alkoxy carbons, whereas the more weakly coupled carbon atoms are the paired peaks. TRAPDOR curves were measured for aluminum isopropoxide as well and show similar behavior. The 14 TRAPDOR curves (not shown) all show different behavior but seem to cluster in groups. This is more clearly visualized in Figure 6, showing the ^{13}C−{^{27}Al} TRAPDOR spectrum compared to the ^{13}C full-echo spectrum (2τ =

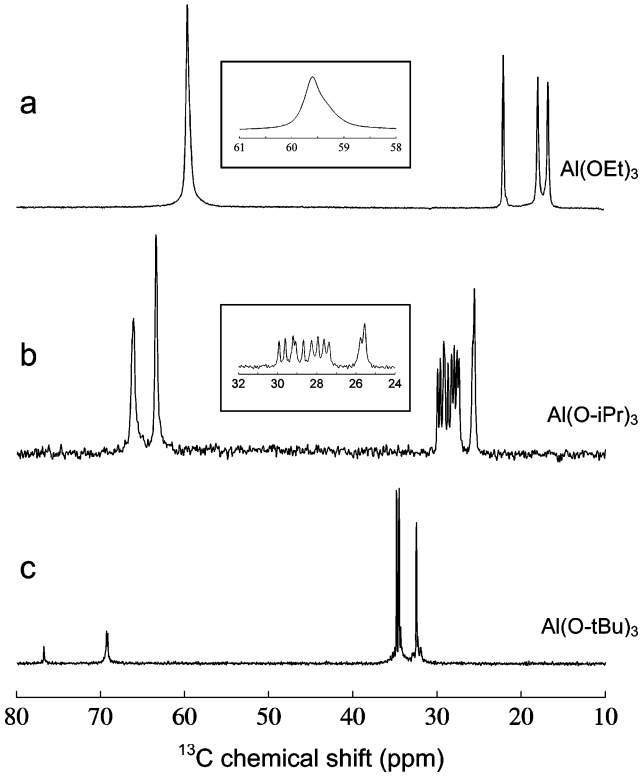

Figure 4. ^{13}C CPMAS NMR spectra of (a) aluminum ethoxide, (b) aluminum isopropoxide, and (c) aluminum *tert*-butoxide. (Inset in a)-Asymmetric line shape of the ethoxy peak. (Inset in b)Enlarged section of the methyl region, clearly showing 11 separate peaks (no line broadening applied in this case). (c) Signal at about 69 ppm is a doublet.

TABLE 2: ^{13}C CPMAS Isotropic Chemical Shifts of Alkoxide Moieties

	δ_{iso} (ppm)
Al−ethoxide	
(CH_3)	21.9, 17.8, 16.6
(OCH_2)	59.6
Al−isopropoxide	
(CH_3) T[a]	29.9, 29.6, 29.2, 29.1, 28.7, 27.6
(CH_3) B[b]	28.3, 27.6, 27.3, 25.8, 25.5[c]
(OCH) T	63.4
(OCH) B	66.1
Al−*tert*-butoxide	
(CH_3) T	34.8, 34.5
(CH_3) B	32.5
(OC) T	69.2, 69.3
(OC) B	76.7

[a] T: carbon atom of terminal alkoxide. [b] B: carbon atom of bridging alkoxide. [c] Contains double intensity.

19.2 ms) of the alkoxy and the methyl regions for aluminum isopropoxide. The TRAPDOR behavior for the methyl groups is indicated on top of each peak (6 weak, 3 intermediate, 3 strong). For the alkoxy-carbon resonance, the resonance at 66 ppm has a much stronger TRAPDOR effect compared to the alkoxy-carbon peak at 63 ppm. In comparing Figure 6 with the inset in Figure 4b, one can see that the spectral resolution in the methyl region is lower in the TRAPDOR experiments then in the ^{13}C VACP MAS spectra. This is due to the fact that the acquisition time was made shorter for all TRAPDOR experiments as compared to the VACP MAS to reduce chances of probe arcing during the experiment, which is especially relevant for the longer echo times.

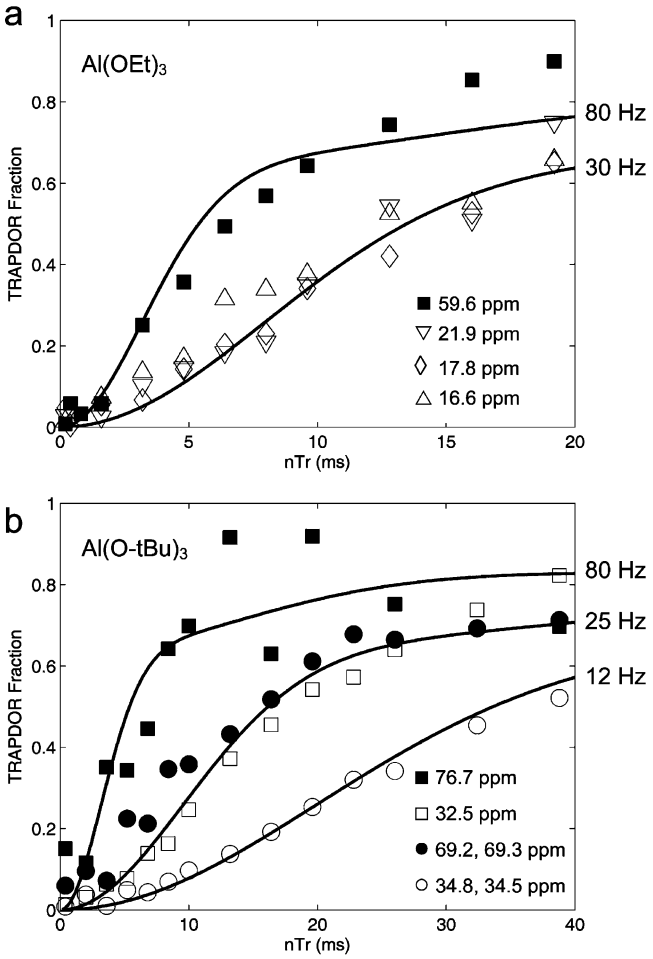

Figure 5. TRAPDOR curves for (a) aluminum ethoxide and (b) aluminum *tert*-butoxide. Solid curves are theoretical curves obtained from the universal REAPDOR curves from ref 31; the dipolar coupling constants used for the curves are indicated to the right of each curve. Filled symbols represent carbons directly attached to oxygen, and the open symbols are the methyl groups. (b) Circles indicate terminal resonances whereas squares represent the carbon atoms part of a bridging butoxide group.

Discussion

To ascertain the structure of these alkoxides, the number of carbon and aluminum species in a sample must be known. These types of compounds form dimers and oligomers, in which terminal and bridging oxygen atoms are present. Hence, the alkyl moiety is attached to either a bridging or a terminal oxygen. Furthermore, there are four possible aluminum coordinations for maintaining charge balance. Aluminum attached to three terminal alkoxides is tri-coordinated aluminum, aluminum coordinated to two terminal and two bridging alkoxides is four-coordinated, aluminum attached to a single terminal and four bridging alkoxides is five-coordinated, and aluminum surrounded by six bridging alkoxy groups is six-coordinated.

Aluminum Tertiarybutoxide. The ^{27}Al MAS and the ^{27}Al MQ-MAS spectra show a single aluminum species with an isotropic chemical shift of 48.5 ppm, indicative of tetrahedral coordination (Figures 2c and 3c, respectively), which suggests a dimeric structure.

In the ^{13}C CPMAS NMR spectrum (Figure 4c), the methyl peaks have a ratio of 1:1:1 and are assigned to three types of methyl-carbon moieties of the *tert*-butoxide moiety. The carbon signals at 76.7, 69.2, and 69.3 ppm with a ratio of 1:1:1 are assigned to three different alkoxy carbons in the crystallographic

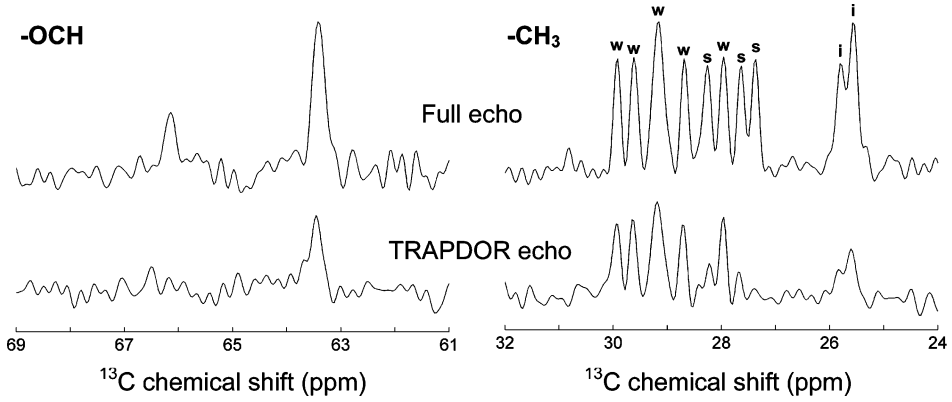

Figure 6. Illustration of the TRAPDOR effect on the methyl (right) and alkoxy region (left) of aluminum isopropoxide. Full-echo spectra are displayed on top, and TRAPDOR echoes are displayed on the bottom. Total echo time was 19.2 ms in all cases. Methyl peaks marked with "w", "i", or "s" indicate a relatively weak, intermediate, and strong TRAPDOR effect, respectively.

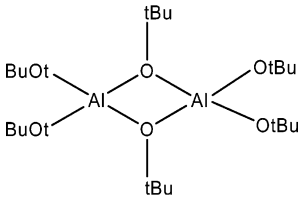

Figure 7. Structure of dimeric aluminum *tert*-butoxide.

TABLE 3: Range of Square Root of the Calculated Heteronuclear $^{13}C-\{^{27}Al\}$ Second Moment for Various Carbons in Aluminum *tert*-butoxide (Hz)

bond type	square root second moment	number of carbons
OC (B)[a]− Al	631−632	2
OC (T)[b]− Al	453−499	4
CH_3 (B) − Al	343−413	6
CH_3 (T) − Al	189−337	12

[a] B: carbon atom of bridging alkoxide. [b] T: carbon atom of terminal alkoxide.

structure. This ratio agrees with the dimeric form proposed by the crystallographic data (Figure 7).[3,13,14]

The $^{13}C-^{27}Al$ TRAPDOR dipolar evolution curves (Figure 5a) clearly show a different behavior for the various resonances. To aid in the assignment and understanding of the different evolution curves, the $^{13}C-\{^{27}Al\}$ heteronuclear second moments were calculated using the heteronuclear van Vleck equation:

$$M_2^{IS} = \frac{1}{4\pi^2}\frac{1}{3}S(S+1)\gamma_I^2\gamma_S^2\hbar^2\left(\frac{\mu_0}{4\pi}\right)\sum\frac{(1-3\cos^2\theta)^2}{r^6}\ (\mathrm{Hz}^2)$$

where S is the ^{27}Al spin quantum number and where $\langle(1-3\cos^2\theta)^2\rangle = (4/5)$ for a powder. Note that in the case of $S = 5/2$, the square root of the second moment would be a factor of $\sqrt{7/3}$ larger than the dipolar coupling D, as used in the universal REAPDOR curve. The values for r_{C-Al} were obtained from crystal structure data. Only C−Al intramolecular distances were used in the calculations as the intramolecular C−Al distances were significantly larger due to the bulky methyl groups, resulting in negligibly weak intermolecular Al−C contacts. Table 3 lists the square root of the second moment for the various carbon atoms. From Table 3 it emerges that the four different types of carbon atoms are well separated in terms of their second moments. The calculated second moment of the bridging methyl carbon was larger than for the terminal methyl carbon. Similarly, the second moment of the bridging secondary carbons was larger than that of the terminal secondary carbon.

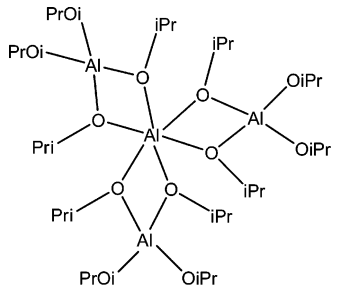

Figure 8. Structure of tetrameric aluminum isopropoxide.

The two inequivalent bridging tertiary carbons have a $\sqrt{M_2}$ of 631 and 632 Hz, whereas the terminal tertiary carbons have a $\sqrt{M_2}$ between 453 and 499 Hz. The second moments of the bridging methyls (343−413 Hz) are overall significantly higher than those of the terminal groups (189−337 Hz). Experimentally, the methyl-carbon peak at 32.5 ppm has a stronger dipolar interaction than the methyl-carbon peaks at 34.5 and 34.8 ppm. Accordingly, the peak at 32.5 ppm was assigned to the bridging *tert*-butoxides, and the peaks at 34.5 and 34.8 ppm were assigned to the terminal *tert*-butoxides. Similarly, the alkoxy-carbon signal at 76.7 ppm was assigned to the bridging *tert*-butoxides, and the tertiary carbon signals at 69.2 and 69.3 ppm were assigned to the terminal *tert*-butoxides, as a stronger dipolar interaction was found for the carbon signal at 76.7 ppm. Hence, all experimental data is in line with a dimeric structure for the aluminum tertiary-butoxide.

Aluminum Isopropoxide. The two peaks with isotropic shifts of around 61.5 and 3.0 ppm are assigned to aluminum atoms in tetrahedral and octahedral coordinations, respectively. Integrating the ^{27}Al MAS spectrum (Figure 2b) peak areas, the ratio of the tetrahedral to the octahedral peak was 3:1. This suggests a tetrameric clustering of aluminum isopropoxide involving six-coordinated aluminum surrounded by 3 four-coordinated aluminum atoms, see Figure 8.[3,13,14]

In the ^{13}C CPMAS NMR spectrum (Figure 4b), the peaks at 63.4 and 66.1 ppm, with a ratio of 1:1, were assigned to two different types of secondary carbons in the crystallographic structure, which is in agreement with a tetrameric structure. The intensities of the 11 resonances from 35 to 20 ppm in the methyl-carbon region of ^{13}C CPMAS spectrum reflect 12 differently crystallographically inequivalent methyl groups in the tetrameric crystallographic structure.[3,13,14] On the basis of intensity ratios and chemical shifts alone, no differentiation of the NMR signals can be made between bridging and terminal groups.

The bridging and terminal isopropoxides in the structure could be identified by their $^{13}C-^{27}Al$ TRAPDOR behavior (Figure

TABLE 4: Range of Square Root of the Calculated Heteronuclear $^{13}C-\{^{27}Al\}$ Second Moment for Various Carbons in Aluminum Isopropoxide (Hz)

bond type	square root second moment	number of carbons
OCH (B)[a]− Al	665−680	6
OCH (T)[b]− Al	469−524	6
$C(1)H_3$ (B) − Al	421−453	6
$C(2)H_3$ (B) − Al	335−340	6
CH_3 (T) − Al	198−258	12[c]

[a] B: carbon atom of bridging alkoxide. [b] T: carbon atom of terminal alkoxide. [c] Structurally, 2 separate methyl groups can actually be discerned, but second moments are too close to make a distinction here.

6). The secondary carbon peak at 66.1 ppm shows stronger dipolar dephasing than the CH carbon peak at 63.4 ppm. In general, both a higher number of aluminum neighbors as well as shorter aluminum−carbon distances will give a stronger dipolar dephasing. Therefore, the alkoxy-carbon peak at 66.1 ppm is assigned to the bridging isopropoxide, and the OCH carbon peak at 63.4 ppm is assigned to the terminal isopropoxide moiety. To be able to analyze the TRAPDOR results more closely, the results of the $^{13}C-\{^{27}Al\}$ second-moment analysis are shown in Table 4. The six bridging secondary carbons have an average $\sqrt{M_2}$ of 673 Hz, while the six terminal secondary carbons have an average $\sqrt{M_2}$ of 496 Hz, which corroborates our assignment.

Among the 12 resonances in the CH_3 region of the spectrum, the three methyl groups resonating at 25.5 and 25.8 ppm (shifted somewhat upfield with respect to the other methyl resonances) showed intermediate dipolar dephasing. The three peaks at 27.3, 27.6, and 28.3 ppm showed an even stronger dipolar dephasing. The remaining six methyl groups showed a weaker coupling to aluminum. This corresponds well with the results of the second-moment analysis based on the crystal structure, where the methyls can be divided in three groups with markedly different second moments. A group of six bridging methyls with $\sqrt{M_2}$ ranging between 421 and 453 Hz represents the three peaks with the strongest TRAPDOR effect (27.3, 27.6, and 28.3 ppm), and another group of six methyls with $\sqrt{M_2}$ ranging between 335 and 340 Hz corresponds to the lines with the intermediate TRAPDOR effect (25.5 and 25.8 ppm). The rest of the six methyl resonances (29.9, 29.6, 29.2, 29.1, 28.7, and 27.6 ppm) have second moments ranging from 198 to 258 Hz, which can be assigned to the terminal methyl carbons. Thus, the NMR data agree well with the reported tetrameric structure of aluminum isopropoxide (Figure 8), even up to the point where a distinction can be made between bridging methyl groups that are slightly bent inward (closer to the six-coordinated aluminum, 27.3, 27.6, and 28.3 ppm) and bridging methyls that are twisted slightly more outward (25.5 and 25.8 ppm).

Aluminum Ethoxide. The ^{27}Al MAS and ^{27}Al MQ-MAS spectra indicate that there is only a single type of aluminum species present (Figures 2a and 3a, respectively). The isotropic chemical shift of 35.5 ppm agrees markedly well with the solution-state value[1] and can be assigned to a five-coordinated species. In the ^{13}C CPMAS NMR spectrum of aluminum ethoxide (Figure 4a), the three resonances of equal intensity (21.9, 17.8, and 16.6 ppm) in the methyl region are assigned to three crystallographically inequivalent methyl groups in the crystal structure. In addition to these, there are two overlapping resonances at 59.6 ppm, which are assigned to two types of methylene carbons attached to the oxygen atom ($-OCH_2-$) of the ethoxide moiety (Figure 4a, inset).

In addition to the ^{13}C chemical shift information, insight into the aluminum ethoxide structure is obtained by evaluating the

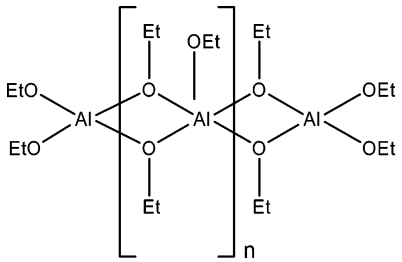

Figure 9. Structure of polymeric aluminum ethoxide.

$^{13}C-\{^{27}Al\}$ TRAPDOR dipolar evolution curve (Figure 5a). All of the methyl-carbon peaks show similar dipolar dephasing behavior. Although the $-OCH_2-$ carbon peak at 59.6 ppm shows a stronger dipolar interaction than that of the methyl carbons, indicating a shorter aluminum−carbon distance, it is to be expected.

There is no X-ray or neutron structure known of the aluminum ethoxide although a tetrameric structure was suggested from solution NMR data[1], indicating the presence of two 4-fold- and two 5-fold-coordinated aluminum atoms. As we observe only 5-fold-coordinated aluminum in the solid state, we propose an analogous structure for solid aluminum ethoxide being a polymer (Figure 9). For such an alkoxide, for each five-coordinated aluminum, there will be four bridging and one terminal oxygen atoms. The tetrahedral coordination of the aluminum atoms at the beginning and the end of the polymer chain are not observed, indicating a very long chain. Although there are indeed 3 separate methyl resonances, based on their similar TRAPDOR curves, it can be concluded that the bridging and the terminal methyls have similar C−Al second moments. The same can be concluded for the bridging and terminal alkoxy carbons, although the chemical shifts do not differ that much.

The TRAPDOR Experiment. The TRAPDOR experiments worked well on these materials, providing enough information to enable the classification of the carbon resonances in terms of bridging and terminal species. The theoretical REAPDOR curves fit some of the data well, whereas, especially at longer echo times, the match was less satisfactory. One reason could be the multi-spin nature of the C−Al interaction in our materials within the same molecule. At longer times, all of the intermolecular dephasing effect start to play a role as well. A further breakdown of the validity of the theoretical curves is the adiabaticity of the level crossings of the aluminum spin under the effect of RF irradiation and magic-angle spinning. To have proper level crossings, the adiabaticity parameter α ($= \nu_{RF}^2/\nu_Q\nu_{MAS}$) should be larger than 0.5. Because the quadrupole couplings constants are large and the RF field strength cannot be too high, α cannot be chosen at liberty. In our case, α was 0.56 for aluminum ethoxide, 0.16 for aluminum *tert*-butoxide, and 0.47 and 3.0 in aluminum isopropoxide for Al(IV) and Al(VI), respectively. A lower α will mean that the level crossings become less adiabatic and fewer aluminum spins will change their state. As a consequence, the TRAPDOR dephasing effect will be reduced for lower values of α and, thus, lead to smaller effective dipolar couplings.

Conclusion

The structures of aluminum ethoxide, aluminum isopropoxide, and aluminum *tert*-butoxide were investigated by means of multinuclear high-resolution and double-resonance solid-state NMR experiments. $^{13}C-^{27}Al$ TRAPDOR experiments were employed successfully to assess the aluminum−carbon dipolar couplings for the alkoxide compounds with Al−O−C connec-

tivities. Furthermore, $^{13}C-^{27}Al$ TRAPDOR experiments were proved to be a very efficient technique for distinguishing between terminal and bridging carbons in aluminum alkoxide structures. The structure of aluminum ethoxide is proposed to be polymeric, containing five-coordinated aluminum. The structures of aluminum isopropoxide and aluminum *tert*-butoxide are confirmed to be tetramer and dimer, respectively.

Acknowledgment. We thank J. W. M. van Os for spoiling the Q of the probe. Technical support from J. W. M. van Os, J. W. G. Janssen, G. E. Jansen, and A. A. K. Klaassen is gratefully acknowledged. The Swiss National Foundation is thanked for their financial support.

References and Notes

(1) Kriz, O. C. B.; Lycka, A.; Fusek, J.; Hermanek, S. *J. Magn. Reson.* **1984**, *60*, 375.
(2) Bradley, D. C. *Adv. Inorg. Chem. Radiochem.* **1972**, *15*, 259.
(3) Fieggen, W.; Gerding, H. *Recueil* **1971**, *90*, 410.
(4) Oliver, J. G.; Worral, I. J. *J. Am. Chem. Soc.* **1970**, *A*, 845.
(5) Lugmair, C. G.; Fujdala, K. L., Tilley, T. D. *Chem. Mater.* **2002**, *14*, 888.
(6) Bradley, D. C. *Metal Alkoxides, Adv. Chem. Series, Am. Chem. Soc.* **1959**, *23*, 10.
(7) Bradley, D. C. *Prog. Inorg. Chem.* **1960**, *2*, 303.
(8) Oliver, J. G.; Phillips, P. K.; Worrall, I. J. *J. Inorg. Nucl. Chem.* **1969**, *31*, 1609.
(9) Fieggen, W.; Gerding, H. *Recueil* **1970**, *89*, 175.
(10) Akitt, J. W.; Duncan, R. H. *J. Magn. Reson.* **1974**, *15*, 162.
(11) Parente, V.; Bredas, J.-L. *Macromol. Theory Simul.* **1996**, *5*, 525.
(12) Lin, C.-H., Ko, B.-T.; Wang, F.-C.; Lin, C.-C.; Kuo, C.-Y. *J. Orgametal. Chem.* **1999**, *575*, 67.
(13) Shiner, V. J.; Whittaker, D.; Fernandez, V. P. *J. Am. Chem. Soc.* **1963**, *85*, 2318.
(14) Akitt, J. W. *Prog. NMR Spec.* **1989**, *21*, 91.
(15) Sugano, T.; Matsubara, K.; Fujita, T.; Takahashi, T. *J. Mol. Catal.* **1993**, *82*, 93.
(16) Ropson, N.; Dubois, Ph.; Jerome, R.; Teyssie, Ph. *Macromolecules* **1993**, *26*, 6378.
(17) Ropson, N.; Dubois, Ph.; Jerome, R.; Teyssie, Ph. *Macromolecules* **1994**, *27*, 5950.
(18) Amoureux, J. P.; Fernandez, C.; Steuernagel, S. *J. Magn. Reson.* **1996**, *123*, 116.
(19) Frydman, L.; Hardwood, J. S. *J. Am. Chem. Soc.* **1995**, *117*, 5367.
(20) Medek, A.; Harwood: J. S.; Frydman, L. *J. Am. Chem. Soc.* **1995**, *117*, 12779.
(21) Grey, C. P.; Vega, A. J. *J. Am. Chem. Soc.* **1995**, *117*, 8232.
(22) Grey, C. P.; Kao, H.-M. *J. Phys. Chem.* **1996**, *100*, 5105.
(23) van Wüllen, L.; Kalwei, M. *J. Magn. Reson.* **1999**, *139*, 250.
(24) Kalwei, M.; Koller, H. *Solid State NMR* **2002**, *21*, 145.
(25) Abragam, A. *The Principles of Nuclear Magnetism*; Oxford University Press: London, 1961.
(26) Detken, A.; Hardy, E. H.; Ernst, M.; Meier, B. H. *Chem. Phys. Lett.* **2002**, 356, 298.
(27) Samoson, A.; Lippmaa, E. *Phys. Rev. B: Condens. Matter Mater. Phys.* **1983**, *28*, 6567.
(28) States, D.; Haberkorn, R.; Ruben, D. *J. Magn. Reson.* **1982**, *48*, 286.
(29) Ernst, R.; Bodenhausen, G.; Wokaun, A. *Principles of Nuclear Magnetic Resonance in One and Two Dimensions*; Oxford University Press: New York, 1987.
(30) MatNMR is a toolbox for processing NMR/EPR data under MATLAB and can be freely downloaded at http://matnmr.sourceforge.net
(31) Goldbourt, A.; Vega, S.; Gullion, T.; Vega, A. J. *J. Am. Chem. Soc.* **2003**, *125*, 11194.